

A bandwidth reconfigurable antenna for devices in low UWB-applications

Mohamed Bikrat^{1,2}, Seddik Bri^{1,2}

¹Material and Instrumentaions: MIN, Electrical Engineering Department, Faculty of Sciences, ESTM - Moulay Ismail University of Meknes, Meknes 50000, Morocco

²Laboratory of Materials Spectrometry and Archaeometry (LASMAR) - Moulay Ismail University of Meknes, Meknes 50000, Morocco

Article Info

Article history:

Received Jul 04, 2022

Revised Dec 20, 2022

Accepted Jan 24, 2023

Keywords:

Band notched

E-shaped slot

PIN diode

Switchable frequency

Ultra-wideband

ABSTRACT

A reconfigurable simple design planar antenna for ultra-wideband applications is proposed, with E-shaped slot contained four narrow vertical slots that has the capacity of switching using four PIN diodes with a ground plan and a microstrip power line. An additional circularly polarized (CP) band is obtained by changing the on/off states of the PIN diodes. Moreover, the four PIN diodes are attached in the middle of the E-shape slot and used to switch the radiation flow of the patch. For validation, a patch antenna design is offered, based on a distinctive situation analysis. The antenna offers the low-ultra-wideband (UWB) frequencies band. Therefore, the switch of the operating states of PIN diodes gives us a good bandwidth re-configurability. In addition, with this flexible configuration we achieve a good -10 dB bandwidths with the ability to change the bandwidth ranges from narrow-band 2.3 GHz to wide-band 3.1 GHz. Also, we achieve a large band for 3 dB AR is 2.57 GHz.

This is an open access article under the [CC BY-SA](https://creativecommons.org/licenses/by-sa/4.0/) license.



Corresponding Author:

Mohamed Bikrat

Material and Instrumentaions: MIN, Electrical Engineering Department, Faculty of Sciences

ESTM - Moulay Ismail University of Meknes, Meknes 50000, Morocco

Email: bikratmed@gmail.com

1. INTRODUCTION

Throughout the last decades, there has been an immense development and progress made in the field of tools and high-tech devices that utilise the not constrained transmitting and receiving antenna, in particular satellite, wireless local-area network (WLAN)/worldwide interoperability for microwave access (WiMAX), and mobile communication as well as radio frequency identification (RFID) communication. These types of antennas [1]–[4], are optimal for either transmitting or receiving signal in accordance with the antenna's operation mechanism, and they are advantageous in terms of low cost, low profile and easy to be mass-produced [5], [6]. The antenna is considered as transmitter in the case radio frequency (RF) energy is radiated, whereas it is viewed as receiver when RF energy is captured in the overall system [7]–[9], therefore, enabling a broader understanding of the role and the scope of ultra-wideband (UWB) devices [10]–[12], and to check the difficulty of wireless communication standards referred to in the literature [13]–[15]. However, the use of spectrum resources from modern wireless communication systems is increasingly stringent [16], [17], requiring the antenna to be expanded to a wider band and more integrated. For body area network (BAN) applications using UWB technologies, as detailed in IEEE 802.15.6 standard [18], [19], and in comparison to other narrow ranges of frequency in [20]–[24].

In this article, a novel bandwidth reconfigurable antenna for WLAN/WiMAX applications is proposed. The reconfiguration technique is introduced to design an antenna controllable in bandwidth using multi-frequency and broadband techniques. We are able to attain three different impedance band widths by

changing the states of the PIN diodes to perform reconfigurability. To achieve a good impedance, a stable radiation pattern throughout the operation states, and good gain.

2. FREQUENCY RESPONSE

The resonance frequency is expressed for the input impedance within the frequency band. The complicated input impedance can be represented by (1).

$$z_{in}(\omega) = R(\omega) + jX(\omega) \quad (1)$$

When $z_{in}(\omega)$ is the complex input impedance, $R(\omega)$ is the resistor, $X(\omega)$ is the radiation frequency and the reactant is. The antenna input impedance determines the reflection coefficient (Γ).

$$\Gamma = (z_{in}(\omega) - Z_0(\omega)) / (z_{in}(\omega) + Z_0(\omega)) \quad (2)$$

We define the "Return Loss" as:

$$\text{Return Loss} = RL = -20 \log \Gamma \quad (3)$$

The bandwidth is closely related with the variation of the impedance which results in the limitation of the frequency range in the radiating element that can be matched to its excitation line [25]. Therefore, this defines the frequency range where the coefficient of reflection is below ≤ -10 dB. In that case, it is enough to determine the value of the frequency corresponding to $S_{11} \leq -10$ dB see Figure 1.

$$BW = fh - fl; S_{11} \leq -10 \text{ dB} \quad (4)$$

$$BW [\%] = 100(fh - fl) / f_{resonance}; S_{11} \leq -10 \text{ dB} \quad (5)$$

According to Hong *et al.* [26], an UWB compact selective frequency surface antenna with high selectivity is any antenna that emits and receives waves with a relative bandwidth $Bfrac$ (fractional bandwidth) greater than or equal to 25%. It is defined as follows with f_c being the center frequency:

$$f_c = (fh - fl) / 2 \quad (6)$$

$$Bfrac = 2(fh - fl) / (fh + fl) = BW / f_c \quad (7)$$

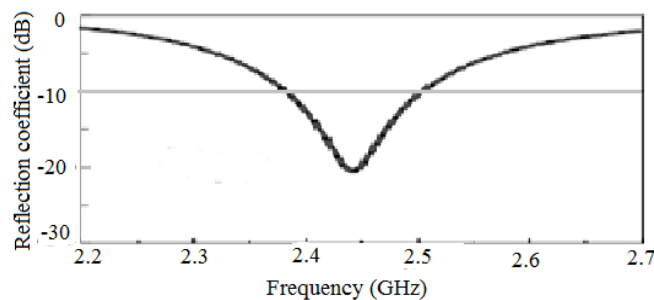


Figure 1. Reflection coefficients of an antenna in dB as a function of the frequency

3. ANTENNA DESIGN

The design is illustrated in Figure 2. It has a (25×50) mm² with a ground dimension of (25×30) mm². The proposed patch consists of a rectangular radiation patch with an E-shaped slot and a four narrow vertical slot, a microstrip supply line and a ground plane. The antenna is designed with an FR4 dielectric substrate with relative permittivity of 4.4 and thickness of 0.8 mm. Four MPP4203 micro semidiodes [27] are attached to the center of the E-shaped slot. They are used as integrated switches between the radiation patch and the E-shape branch besides, they act as bridge for the current flow between the E-shape and the four rectangles. The antenna was simulated using the commercial Ansoft high-frequency structure simulator (HFSS). The HFSS is used to perform this design and in the optimization process. The final parameters are $L_s = 50$ mm, $W_1 = 1.3$ mm, $L_3 = 1.5$ mm, $L_1 = 8$ mm, $W_4 = 18.5$ mm, $W_3 = 1$ mm, $L_g = 30$ mm, $W_s = 25$ mm, $L_2 = 1$ mm, $L_4 = 15.5$ mm, $L_5 = 1.5$ mm, $W_2 = 1.5$ mm, $W_5 = 0.2$ mm.

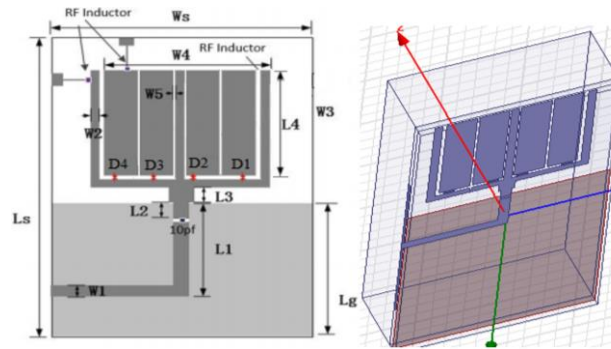


Figure 2. Structure of the proposed antenna

4. RESULTS AND INTERPRETATIONS

We change the operational status of four PIN diodes to see the scalable procedure frequency response of the reflective bandwidth of -10 dB. Figure 3 demonstrates the scalable procedure for the proposed antenna. By changing the working state of the PIN diodes to 4.5 GHz. First, when all four PIN diodes are enabled, the antenna reverberates to 4.38 GHz. The distribution of surface current circulates mostly along the E-shape branch, which is similar to a monopole antenna. It generates only one relatively narrow impedance bandwidth that is 3.3 GHz, with one resonant frequency at 4.38 GHz. When the right PIN diode D1 is switched off, the bandwidth of -10 dB covers the frequency band from 2.7 GHz to 5.1 GHz, with an impedance bandwidth of 2.4 GHz.

While the PIN diode D2 is turned off; the antenna resonates at 4.33 GHz. It has a relatively narrow impedance bandwidth with 2.05 GHz. However, when D3 is turned off, shows that the simulated impedance bandwidths cover the frequencies band from 2.6 GHz to 5.04 GHz. But for D4 is turned off the response of impedance bandwidths cover a large band of frequencies from 1.9 GHz to 5.1 GHz.

Figure 4 shows the antenna performance for various PIN diodes states, with two diodes are turned off everytime, which gives the following results:

- When D1 and D2 PIN diodes are off, the frequency response moves to high frequency at 4.1 GHz and at 2.4 GHz.
- When D2 and D3 PIN diodes are off, the -10 dB reflection bandwidth presents in the band of frequencies from 2.62 GHz to 5.1 GHz with large impedance band of 2.38 GHz.
- When D3 and D4 PIN diodes are off, response of the -10 dB reflection bandwidth stills the same
- When D4 and D1 PIN diodes are off, but antenna resonant change to 2.3 GHz.

We observe that when choose to turn off one diode every time simultanly, we get different resonance frequency for each case. Besides that, the bandwidth almost still the same for all cases. Indeed, we conclude that the switching-off of diodes from D1 to D4 allow our patch antenna to perform with many resonance frequencies begin with 2 GHz up to 5.1 GHz.

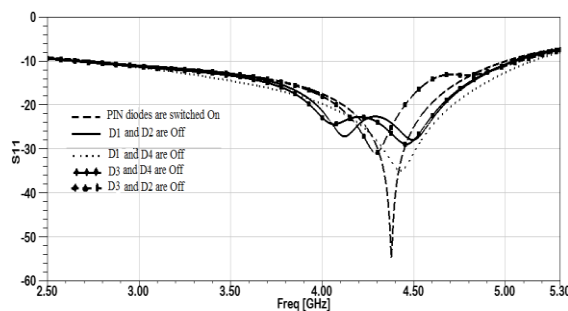


Figure 3. Reflection coefficients of the proposed antenna with feeding frequency at 4.5 GHz

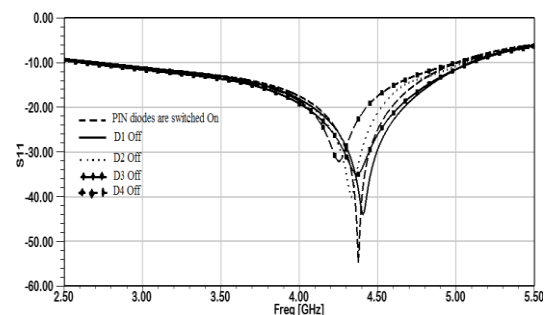


Figure 4. Reflection coefficients of the proposed antenna with feeding frequency at 4.5 GHz

In Figure 5 we present the frequency response of the evolving -10 dB reflection bandwidth procedure, for different situation of PIN diodes.

- D1 is on, the -10 dB reflection bandwidth is 2.72 GHz, with resonant frequency around 4.7 GHz.

- D2 is on; response of the -10 dB reflection bandwidth is 2.8 GHz.
- D3 is on, the reflection bandwidth of -10 dB present in the band the frequencies from 2.55 GHz to 5.22 GHz and with large band of 2.73 GHz.
- D4 is on, however, response of the -10 dB reflection bandwidth is 2.65 GHz.

In this step we choose to turn off two diodes for every case. In which we achieve multi resonance frequencies for two first cases (D1 is on) instead of the last towcases (D4 is on) when we get only one resonance frequency. Which give us a flexible use of our patch antenna.

Figure 6 shows the simulation result forthe reflection bandwidth of the proposed antenna. To be precise:

- When the four PIN diodes are activated, antenna resonates at 4.38 GHz. Moreover, it has an impedance bandwidth of 2.5 GHz.
- When the four PIN diodes are off, the -10 dB reflection band response covers a relatively narrow frequency band of 2 GHz 5.1 GHz.

In the opposite of the first step in Figure 2, we chose to turn on this time one diode everytime. At this step we get many separated resonance frequency for each case rather than the first step in witch we get approached resonance frequencies. Indeed, we see that step shows that our antenna could performe better than the first step.

Figure 7 presents the -3 dB augmented reality (AR) bandwidths simulation result for different state of PIN diodes. However:

- When the four PIN diodes are off, the simulated axial ratio bandwidth (ARBW) of 3 dB covers a narrow band of frequencies from 3.55 GHz to 3.68 GHz and a broad band of frequencies from 4.49 GHz to 4.67 GHz.
- When the four PIN diodes are turned on, the axial ratio bandwidth response of 3 dB covers a narrow band of frequencies from 3.52 GHz to 4.08 GHz and a broad band of frequencies from 4.69 GHz to 4.87 GHz.

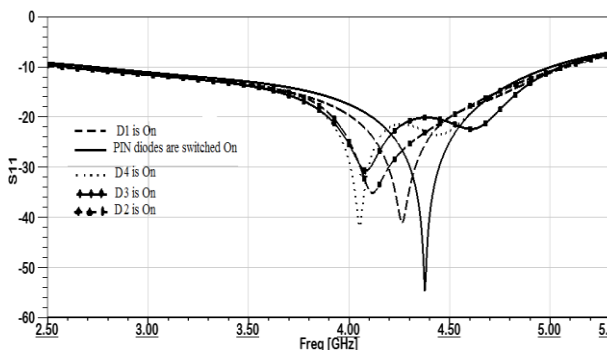


Figure 5. Reflection coefficients of the proposed antennawith feeding frequencyat 4.5 GHz

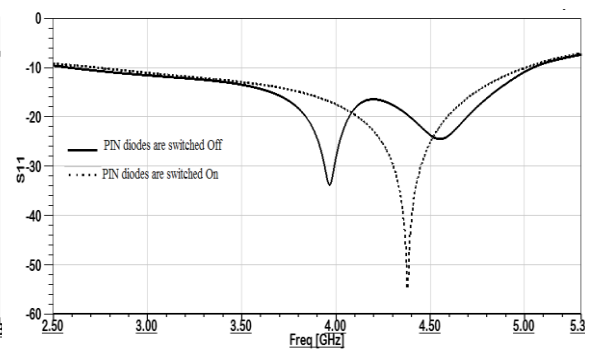


Figure 6. Reflection coefficients of the proposed antennawith feeding frequency at 4.5 GHz

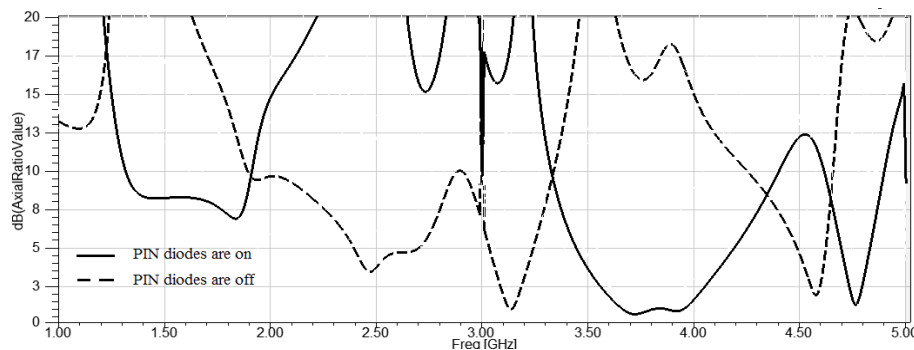


Figure 7. AR bandwidths of the proposed antennawith feeding frequency at 4.5 GHz

The proposed antenna circuit topology is determined by its geometry, frequency, and environment. Figure 8 shows the cell number for the equivalent circuitry. The number of cells is determined by the number of the input impedance local maxima as seen in Figure 9. However, the input cell (C_0 and L_0) is calculated using the imaginary part of the input impedance plot of the antenna simulated, and we can calculate the components ($R_i L_i C_i$) of each cell ($i = 1, 2, \dots, N$) from the real part of the input impedance of antenna in the air [28].

Table 1 illustrates the patch equivalent circuit parameters; we observe that the number of components of each cell corresponds to the state of PIN diodes. Moreover, the components $(R_i L_i C_i)$ of the three cells are influenced when all the diodes are powered off. Equally; we noted that out of the three cells, cells 2 and 3 are the most affected by the change in the status of diodes. Meanwhile, input cell (C_0, L_0) is almost unaffected and can be said to be independent of status of PIN diodes.

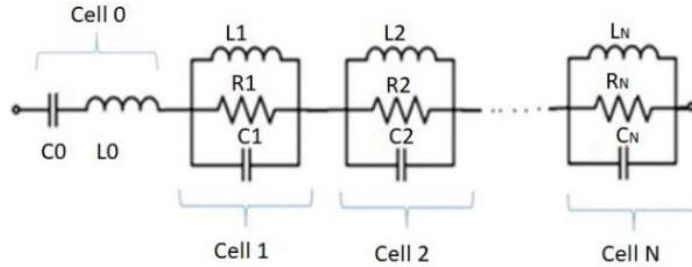


Figure 8. Topology of the equivalent circuit of the proposed antenna

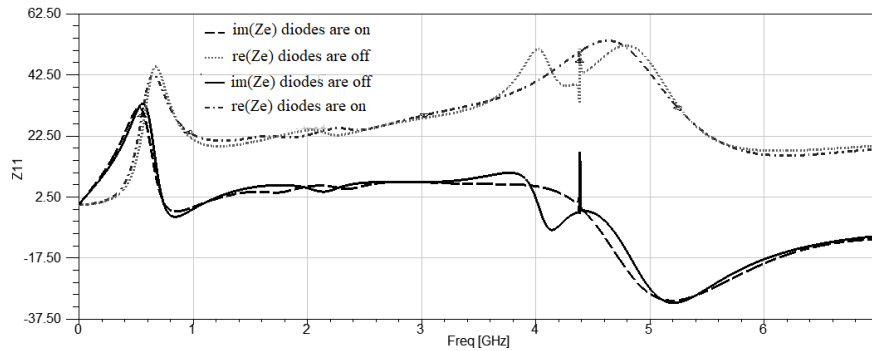


Figure 9. Real and imaginary parts of the input impedance of the antenna

Table 1. Antenna equivalent circuit parameters as a switch the operating state of four PIN diodes

States of PIN	Circuit parameter										
	C_0 (pF)	L_0 (nH)	C_1 (pF)	L_1 (nH)	R_1 (Ω)	C_2 (pF)	L_2 (nH)	R_2 (Ω)	C_3 (pF)	L_3 (nH)	R_3 (Ω)
Off	1.34	0.23	13.03	0.181	53	12.98	0.178	51	13.1	0.179	52.5
On	1.35	0.21	16.95	0.16	43	13.18	0.185	55	-	-	-

Figure 10(a), Figure 10(b), Figure 11(a), and Figure 11(b) are showing the simulated radiation patterns E-plan and H-plan foretow different modes. The radiation patterns for these states in the xz -plane are almost unaffected, so they are not shown for brevity. We can see that the level of cross-polarisation is very small.

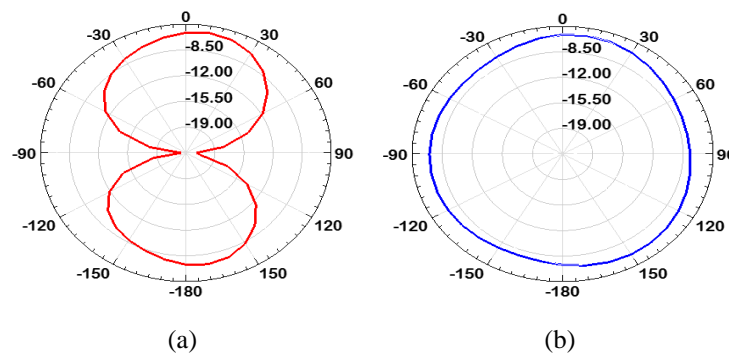


Figure 10. Radiation patterns of the proposed antenna when the four PIN diodes are on: (a) E side (YOZ) and (b) H side (XOZ)

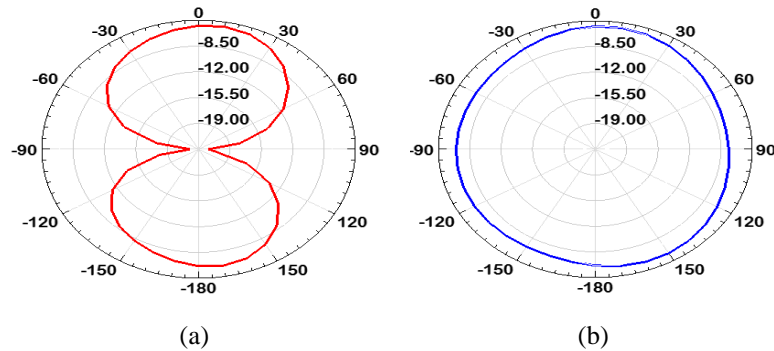


Figure 11. Radiation patterns of the proposed antenna when the four PIN diodes are off: (a) E side (YOZ) and (b) H side (XOZ)

5. SURFACE CURRENT DISTRIBUTION

In Figure 12, the surface current's distribution of different states of four PIN diodes are mentioned. When the four PIN diodes are turned off at 4.5 GHz, it shows that the majority of the surface current spread from the bottom of the patch to the border and middle. That's to say, the current's density is most focused around the E-shaped slot and the center of the patch at edge of the patch as Figure 12(a). When all the four PIN diodes are turned on at 4.5 GHz, it shows that the majority of the surface current spreads from the bottom of the patch in four narrow vertical slots to the center of the patch. Moreover, the weak current is located along the border in E-shap and the four rectangles as Figure 12(b).

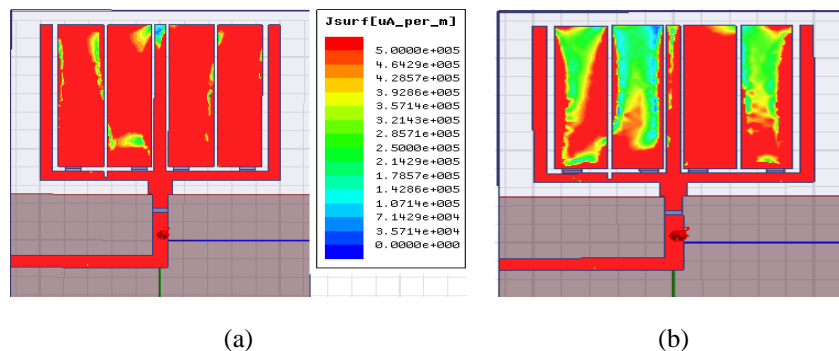


Figure 12. Surface current distributions (a) the four PIN diodes are switched off and (b) the four PIN diodes are switched at 4.5 GHz

6. COMPARISON

Table 2 provides a comparative summary of the recently proposed bandwidth reconfigurable antenna types published previously. The proposed antenna's performance is compared with the other referred to antennas for the low-UWB frequencies band applications [29]–[32]. We came to the conclusion that our proposed antenna offers appropriate gains to enough bandwidths to cover the narrow-band and wide-band within a small size simple structure.

We noted that our simulation result achieved better response than all results that were before and we had a large band that can reach up to 3.1 GHz (2–5.1 GHz) with reflection coefficient value of -56 dB, as mentioned in the comparative table simulation, especially when we observe the resonance frequency in the narrow-band and wide-band either cover all low-UWB frequencies band. In addition, this promising result comes as result of working with several states of PIN diodes, unlike what the previously published works opted for. Whereas, other published works antennas do not exceed 1.7 GHz inband and -35 dB in gain according to previous works [30]. Particularly results from article [32], the evolutionary procedure frequency response of the impedance bandwidth ranges from 5.65 GHz to 5.9 GHz, and reflection coefficient value is -34.08 dB, based on this result we can model and design a new antenna with new geometry such as C-shaped slot in order to get a large wide-band. Therefore, it is concluded that our work demonstrates good performance overall in terms of the gain and size as well as 3 dB ARBW and the -10 dB reflection bandwidth.

Table 2. Performance comparison of polarized antennas

References	Substrate size (mm ³)	Notching structure	Band low-UWB (GHz)	Reflection coefficient (dB)
[29]	40×30×0.787	U-slot	5.1–5.8	-34
[30]	19×19×1.6	Microstrip-fed circular monopole antenna	4.36–6.06	-35
[31]	49.4×49.4×1.9	E-shaped fractal	3.23–3.65	-29
[32]	26×22×0.21	Microstrip antenna array	5.65–5.9	-34.08
This work	25×30×0.8	Four narrow vertical and E-shaped slot	2–5.1	-56

7. CONCLUSION

The reconfigurable bandwidth antenna has a rectangular radiation patch connected to a micro strip power line with an E-shaped slot and a truncated ground plane on the back of an FR-4 substrate. Two PIN diode pairs at the middle of the slot on the radiation patch control the current flow. The proposed antenna design was reviewed to determine the reconfigurability of the frequencies; as a effect, the performance of the antenna was satisfactorily compared to the recently released reconfigurable bandwidth antenna types. The result shows that by changing the working states of the diodes, the characteristic frequency bandwidth of the antenna can be reconfigured from narrowband to wideband. The impedance bandwidth ranges from narrow-band 2.3 GHz to wide-band 3.1 GHz with reflection coefficient value of -56 dB, thus our proposed antenna has a good ability for several protocols of wireless communication technologies, such as fifth generation (5G), satellite communication, WLAN, and WiMAX. Moreover, we worked with four diodes, which give us the opportunity to have a flexible configuration in order to get switchable bandwidth with many resonances frequencies, and the ability to manipulate and control electromagnetic behaviour. As result, this new conception is adequate with many different bands and has good isolation between different wireless standards with the following advantages: simple integration, low cost, lite weight.




REFERENCES

- [1] H. A. Majid, M. K. A. Rahim, M. R. Hamid, N. A. Murad, and M. F. Ismail, "Frequency-reconfigurable microstrip patch-slot antenna," *IEEE Antennas and Wireless Propagation Letters*, vol. 12, pp. 218–220, 2013, doi: 10.1109/LAWP.2013.2245293.
- [2] A. -F. Sheta and S. F. Mahmoud, "A widely tunable compact patch antenna," *IEEE Antennas and Wireless Propagation Letters*, vol. 7, pp. 40–42, 2008, doi: 10.1109/LAWP.2008.915796.
- [3] B. A. Cetiner, G. R. Crusats, L. Jofre, and N. Biyikli, "RF MEMS integrated frequency reconfigurable annular slot antenna," *IEEE Transactions on Antennas and Propagation*, vol. 58, no. 3, pp. 626–632, 2010, doi: 10.1109/TAP.2009.2039300.
- [4] M. Gholamrezaei, F. Geran, and R. A. Sadeghzadeh, "Completely independent multi-ultrawideband and multi-dual-band frequency reconfigurable annular sector slot antenna (FR-ASSA)," *IEEE Transactions on Antennas and Propagation*, vol. 65, no. 2, pp. 893–898, 2017, doi: 10.1109/TAP.2016.2632726.
- [5] S. -L. S. Yang, A. A. Kishk, and K. -F. Lee, "Frequency reconfigurable U-slot microstrip patch antenna," *IEEE Antennas and Wireless Propagation Letters*, vol. 7, pp. 127–129, 2008, doi: 10.1109/LAWP.2008.921330.
- [6] H. -Y. Li, C. -T. Yeh, J. -J. Huang, C. -W. Chang, C. -T. Yu, and J. -S. Fu, "CPWfed frequency-reconfigurable slot-loop antenna with a tunable matching network based on ferroelectric varactors," *IEEE Antennas and Wireless Propagation Letters*, vol. 14, pp. 614–617, 2015, doi: 10.1109/LAWP.2014.2375334.
- [7] R. B. V. B. Simorangkir, Y. Yang, K. P. Esselle, and B. A. Zeb, "A method to realize robust flexible electronically tunable antennas using polymerembedded conductive fabric," *IEEE Transactions on Antennas and Propagation*, vol. 66, no. 1, pp. 50–58, 2018, doi: 10.1109/TAP.2017.2772036.
- [8] Y. Kabalci, I. Develi, and E. Kabalci, "LDPC coded OFDM systems over broadband indoor power line channels: A performance analysis," in *4th International Conference on Power Engineering, Energy and Electrical Drives*, 2013, pp. 1581–1585, doi: 10.1109/PowerEng.2013.6635852.
- [9] S. W. Wong, Z. -C. Guo, K. Wang, and Q. -X. Chu, "A compact tunable notched-band ultra-wide-band antenna using a varactor diode," in *Proceedings of 2014 3rd Asia-Pacific Conference on Antennas and Propagation*, 2014, pp. 161–163, doi: 10.1109/APCAP.2014.6992440.
- [10] S. -Y. Chen and Q. -X. Chu, "A reconfigurable dual notched-band UWB antenna," in *2015 IEEE 4th Asia-Pacific Conference on Antennas and Propagation (APCAP)*, 2015, pp. 103–104, doi: 10.1109/APCAP.2015.7374289.
- [11] D. E. Anagnostou and A. A. Gheethan, "A coplanar reconfigurable folded slot antenna without bias network for WLAN applications," *IEEE Antennas and Wireless Propagation Letters*, vol. 8, pp. 1057–1060, 2009, doi: 10.1109/LAWP.2009.2031989.
- [12] H. Alsariera *et al.*, "Simple broadband circularly polarized monopole antenna with two asymmetrically connected U-shaped parasitic strips and defective ground plane," *TELKOMNIKA (Telecommunication Computing Electronics and Control)*, vol. 18, no. 3, pp. 1169–1175, 2020, doi: 10.12928/telkomnika.v18i3.14313.
- [13] T. Aboufoul, C. Parini, X. Chen, and A. Alomainy, "Pattern-reconfigurable planar circular ultra-wideband monopole antenna," *IEEE Transactions on Antennas and Propagation*, vol. 61, no. 10, pp. 4973–4980, 2013, doi: 10.1109/TAP.2013.2274262.
- [14] M. M. H. Mahfuz, M. S. Islam, I. M. Rafiqul, M. H. Habaebi, and N. Sakib, "Design of UWB microstrip patch antenna with variable band notched characteristics," *TELKOMNIKA (Telecommunication Computing Electronics and Control)*, vol. 19, no. 2, pp. 357–363, 2021, doi: 10.12928/telkomnika.v19i2.18147.
- [15] T. Otim, P. L. -Iturri, L. Azpilicueta, A. Bahillo, L. E. Diez, and F. Falcone, "A 3D ray launching timefrequency channel modeling approach for UWB ranging applications," *IEEE Access*, vol. 8, pp. 97321–97334, 2020, doi: 10.1109/ACCESS.2020.2996408.
- [16] P. A. Catherwood, S. S. Bukhari, G. Watt, W. G. Whittow, and J. McLaughlin, "Body-centric wireless hospital patient monitoring networks using body-contoured flexible antennas," *IET Microwaves, Antennas & Propagation*, vol. 12, no. 2, pp. 203–210, 2018, doi: 10.1049/iet-map.2017.0604.
- [17] A. Maunder, O. Taheri, M. R. G. Fard, and P. Mousavi, "Calibrated layer-stripping technique for level and permittivity measurement with UWB radar in metallic tanks," *IEEE Transactions on Microwave Theory and Techniques*, vol. 63, no. 7, pp. 2322–2334, 2015,




- doi: 10.1109/TMTT.2015.2429141.
- [18] H. Khani and H. Nie, "Near-optimal detection of monobit digitized UWB signals in the presence of noise and strong intersymbol interference," *IEEE Systems Journal*, vol. 14, no. 2, pp. 2311–2322, 2020, doi: 10.1109/JSYST.2019.2925930.
- [19] S. Wang, G. Mao, and J. A. Zhang, "Joint time-of-arrival estimation for coherent UWB ranging in multipath environment with multi-user interference," *IEEE Transactions on Signal Processing*, vol. 67, no. 14, pp. 3743–3755, 2019, doi: 10.1109/TSP.2019.2916016.
- [20] M. S. Mohammadi, E. Dutkiewicz, Q. Zhang, and X. Huang, "Optimal energy efficiency link adaptation in IEEE 802.15.6 IR-UWB body area networks," *IEEE Communications Letters*, vol. 18, no. 12, pp. 2193–2196, 2014, doi: 10.1109/LCOMM.2014.2364226.
- [21] I. Elfergani, J. Rodriguez, I. Otung, W. Mshwat, and R. A. -Alhameed, "Slotted printed monopole UWB antennas with tunable rejection bands for WLAN/WiMAX and X-Band coexistence," *Radioengineering*, vol. 27, no. 3, pp. 694–702, 2018, doi: 10.13164/re.2018.0694.
- [22] H. Ullah and F. A. Tahir, "A high gain and wideband narrow-beam antenna for 5G millimeter-wave applications," *IEEE Access*, vol. 8, pp. 29430–29434, 2020, doi: 10.1109/ACCESS.2020.2970753.
- [23] T. Li and Z. N. Chen, "Compact wideband wide-angle polarization-free metasurface lens antenna array for multibeam base stations," *IEEE Transactions on Antennas and Propagation*, vol. 68, no. 3, pp. 1378–1388, 2020, doi: 10.1109/TAP.2019.2938608.
- [24] M. Bikrat and S. Bri, "A Bandwidth Reconfigurable Planar Antenna for UWB-Applications," *E3S Web Conference*, vol. 351, pp. 1-5, 2022, doi: 10.1051/e3sconf/202235101060.
- [25] S. -D. Xu *et al.*, "A Wide-Angle Narrowband Leaky-Wave Antenna Based on Substrate Integrated Waveguide-Spoof Surface Plasmon Polariton Structure," *IEEE Antennas and Wireless Propagation Letters*, vol. 18, no. 7, pp. 1386–1389, 2019, doi: 10.1109/LAWP.2019.2917561.
- [26] T. Hong, M. Wang, K. Peng, Q. Zhao, and S. Gong, "Compact ultra-wide band frequency selective surface with high selectivity," *IEEE Transactions on Antennas and Propagation*, vol. 68, no. 7, pp. 5724–5729, 2020, doi: 10.1109/TAP.2020.2963905.
- [27] "Data sheet of MPP4203 PIN diodes," *Microsemi*. <http://www.microsemi.com> (accessed Feb. 21, 2019).
- [28] M. Ansarizadeh, A. Ghorbani, and R. A. A. -Alhameed, "An approach to equivalent circuit modeling of rectangular microstrip antennas," *Progress In Electromagnetics Research B*, vol. 8, pp. 77–86, 2008, doi: 10.2528/PIERB08050403.
- [29] S. Wang, K. Li, F. Kong, and L. Du, "A miniaturized triple-band planar antenna combing single-cell metamaterial structure and defected ground plane for WLAN/WiMAX applications," *Journal of Electromagnetic Waves and Applications*, vol. 35, no. 3, pp. 357–370, 2021, doi: 10.1080/09205071.2020.1839569.
- [30] S. Gupta, S. Patil, C. Dalela, and B. K. Kanaujia, "Analysis and design of inclined fractal defected ground-based circularly polarized antenna for CA-band applications," *International Journal of Microwave and Wireless Technologies*, vol. 13, no. 4, pp. 397–406, 2021, doi: 10.1017/S1759078720001142.
- [31] M. T. Ali, H. Jaafar, S. Subahir, and A. L. Yusof, "Gain enhancement of air substrates at 5.8GHz for microstrip antenna array," in *2012 Asia-Pacific Symposium on Electromagnetic Compatibility*, 2012, pp. 477–480, doi: 10.1109/APEMC.2012.6237872.
- [32] S. -Y. Chen, Q. -X. Chu, and N. Shinohara, "A bandwidth reconfigurable planar antenna for WLAN/WiMAX applications," in *2016 Asia-Pacific Microwave Conference (APMC)*, 2016, pp. 1–3, doi: 10.1109/APMC.2016.7931467.

BIOGRAPHIES OF AUTHORS



Mohamed Bikrat    Ph. D student in electrical engineering from the University of Mekens, Morocco. Received the master's degree in engineering science from the University of Kenitra, Morocco, in 2019 and the bachelor's degree in electrical engineering from the University of Oujda, Oujda, Morocco, in 2014. He can be contacted at email: bikratmed@gmail.com.



Seddik Bri    He is currently a professor at the High School of Technology (ESTM), Moulay Ismail University, Meknes, Morocco. His scientific work interested on material characterisation, patch antenna, the microwaves' applications and the security in communications systems. He can be contacted at email: briseddik@gmail.com.